Energy Compression and Stabilization of Laser-Plasma Accelerators

A. Ferran Pousa,[1,*] I. Agapov,[1] S. A. Antipov,[1] R. W. Assmann,[1,2] R. Brinkmann,[1]
W. P. Leemans,[1,3] A. Martinez de la Ossa,[1] J. Osterhoff,[1] and M. Thévenet[1]

[1] *Deutsches Elektronen-Synchrotron DESY, Notkestraße 85, 22607 Hamburg, Germany*
[2] *Laboratori Nazionali di Frascati, Via Enrico Fermi 40, 00044 Frascati, Italy*
[3] *Department of Physics Universität Hamburg, Luruper Chaussee 149, 22761 Hamburg, Germany*

(Dated: June 3, 2021)

Laser-plasma accelerators (LPAs) outperform current radiofrequency technology in acceleration strength by orders of magnitude. Yet, enabling them to deliver competitive beam quality for demanding applications, particularly in terms of energy spread and stability, remains a major challenge. In this Letter, we propose to combine bunch decompression and active plasma dechirping for drastically improving the energy profile and stability of beams from LPAs. Start-to-end simulations demonstrate the efficacy of such post-acceleration phase-space manipulations and the potential to reduce current state-of-the-art energy spread and jitter from 1 % to 0.10 % and 0.024 %, respectively, closing the beam-quality gap to conventional acceleration schemes.

Laser-plasma accelerators (LPAs) [1] have attracted considerable attention in recent years due to their potential for realizing ultra-compact particle accelerators. Among many applications, they could enable a new generation of cost-effective coherent light sources [2] or injectors for future storage rings [3]. Landmark achievements such as the generation of electron beams with peaked energy spectrum [4–6], GeV energy [7–9], high current [10] and low emittance [11–13], have brought the performance of these devices closer to current radiofrequency accelerators. However, numerous challenges still limit their applicability, in particular with regards to the beam energy spread and stability.

Achieving a low ($\lesssim 0.1\,\%$) energy spread is especially relevant for applications such as free-electron lasers [14]. Although large efforts have been made to minimize it, beams from LPAs still typically exhibit $\gtrsim 1\,\%$ energy spreads [15]. One of the main reasons for this is the large slope of the accelerating fields, which leads to a strong longitudinal energy correlation (chirp) along the accelerated beams. This slope can be flattened by means of beam loading [16–18], which has allowed the demonstration of 1 % to 10 % energy spreads [15, 19]. The remaining energy spread arises from non-linear correlations as well as the intrinsic slice energy spread [20], which can arise from the betatron motion of beam particles [21]. Several concepts can also mitigate the energy spread when beam loading is negligible [22–24], but are therefore limited in charge and efficiency. Alternatively, plasma dechirpers [25–28] and dielectric [29, 30] or corrugated [31, 32] structures could passively reduce the energy spread after acceleration by means of beam self-generated wakefields.

In addition to a low energy spread, a high energy stability is required for most applications. In particular, injectors for diffraction-limited storage rings require both an energy spread and energy jitter well below the momentum acceptance of the ring (typically $\sim 1\,\%$ [33]) in order to minimize charge losses. Currently, with a state-of-the-art energy jitter $> 1\,\%$ rms [34], LPAs operate an order of magnitude above this requirement. A promising path towards improved stability is the use of advanced machine-learning techniques [35] and active feedback systems with high-repetition-rate (kHz) lasers. These have been successfully implemented to stabilize the driver [36] as well as optimizing and stabilizing the parameters of the output beams [37, 38], even at moderate repetition rates [35, 39]. Such techniques could prove essential for realizing reliable LPAs, but might not be sufficient for reaching $\lesssim 0.1\,\%$ energy spread and jitter levels.

In this Letter, we propose to combine bunch decompression and active plasma dechirping for drastically reducing the energy spread *and* energy jitter of LPAs. The decompression, performed by a magnetic chicane, imprints a linear correlation between the arrival time and the energy of the beam particles [40]. An *active* plasma dechirper (APD), in which a wakefield is generated by a fraction of the LPA laser driver, is then able to correct deviations with respect to the target energy thanks to the imprinted correlation and the intrinsic synchronization between the LPA and APD drivers. Contrary to *passive* dechirpers [25–28], an APD can correct not only the beam energy spread but also the central energy jitter. All together, the decompression and dechirping result in a system for energy compression [41] and stabilization which, unlike in previous work [24], is only applied after acceleration and is not limited to weakly beam-loaded LPAs. Thus, it could be incorporated into current state-of-the-art setups [15, 35] to further improve the energy spread and achieve an unprecedented energy stability. Start-to-end simulations with the FBPIC [42] and OCELOT [43] codes demonstrate its feasibility. This scheme, originally outlined in [44], further highlights the utility of dispersive media for improving the performance of high-gradient accelerators [24, 40, 45–47].

The combined effect of decompression and dechirping can be studied by investigating the single-particle dynamics. By establishing a reference energy γ_{ref} as the desired beam energy of the accelerator, a relative energy

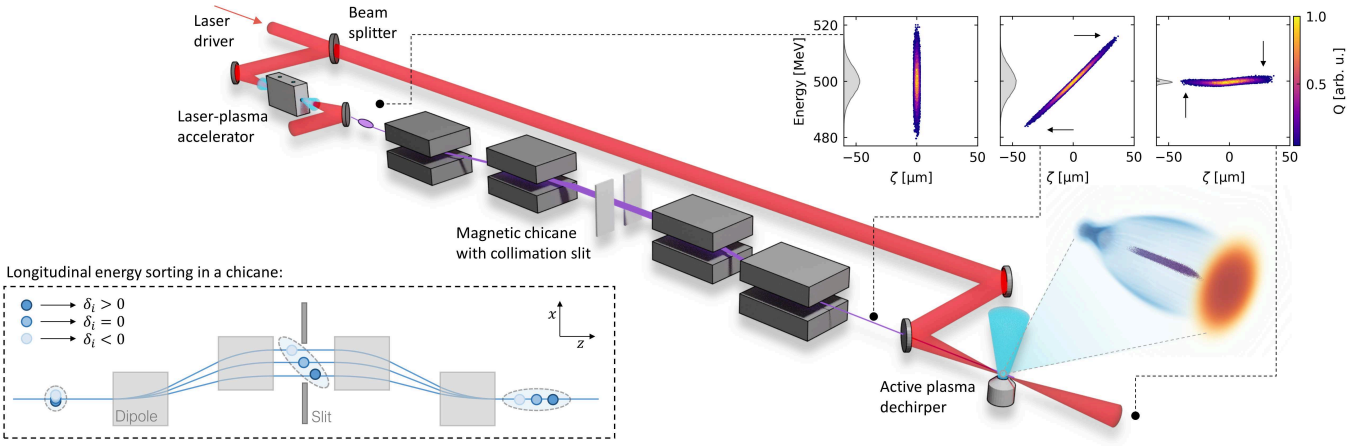

FIG. 1. Basic layout and working principle of an LPA energy compressor and stabilizer. Only the LPA source and the relevant beam line components (laser, chicane and APD) are shown. The longitudinal phase space of the beam at different locations is also displayed, as well as the 3D [48] wakefield structure in the APD.

deviation $\delta(t) = (\gamma(t) - \gamma_{\rm ref})/\gamma_{\rm ref}$ and longitudinal coordinate $\zeta(t) = z(t) - z_{\rm ref}(t)$ can be defined for each particle. Here, $\gamma = \sqrt{1 + (\mathbf{p}/m_e c)^2}$ is the relativistic Lorentz factor, with $\mathbf{p}$ and m_e being, respectively, the momentum and rest mass of an electron; c is the speed of light in vacuum; t is time; z is the longitudinal position; and $z_{\rm ref}$ is the position of a reference particle with $\delta = 0$ initially located at the beam center. A dispersive section transforms the phase-space coordinates of a particle initially at $(\zeta_i,\, \delta_i)$ to a final position $\zeta_f = \zeta_i + R_{56}\delta_i + \mathcal{O}(\delta_i^2)$ [49], where R_{56} is the linear dispersion coefficient, while leaving the energy unchanged. Thus, to first order in δ_i, a beam with no initial correlation between ζ_i and δ_i is longitudinally stretched by a factor

$$S \equiv \frac{\sigma_{\zeta_f}}{\sigma_{\zeta_i}} = \sqrt{\left(\frac{R_{56}\sigma_{\delta_i}}{\sigma_{\zeta_i}}\right)^2 + 1}\ , \tag{1}$$

while developing a linear chirp $\chi \equiv \sigma_{\zeta\delta}/\sigma_\zeta^2 = R_{56}^{-1}(1 - S^{-2})$, which is $\chi \simeq R_{56}^{-1}$ for $S^2 \gg 1$. Here σ_ζ and σ_δ are the standard deviations of ζ and δ, and $\sigma_{\zeta\delta}$ is their covariance. After decompression, the beam enters a dechirper of length L which applies a linear longitudinal electric field $E_z(\zeta) = -(m_e c^2/e)\mathcal{E}'(\zeta - \zeta_0)$ with normalized slope $\mathcal{E}'$ centered at ζ_0, where e is the elementary charge. This leaves the position of the particles unchanged, but transforms their energy into a final value

$$\delta_f = \frac{1}{R_{56}}(\zeta_f - \zeta_i) + \frac{\mathcal{E}' L}{\gamma_{\rm ref}}(\zeta_f - \zeta_0)\ . \tag{2}$$

Eq. (2) shows that the energy correlation imprinted by the linear dispersion can be compensated for by the dechirper if

$$\mathcal{E}' L = -\frac{\gamma_{\rm ref}}{R_{56}}\ . \tag{3}$$

This results in a net reduction of the beam energy spread, which is fully determined by R_{56} as

$$\sigma_{\delta_f} = \frac{\sigma_{\zeta_i}}{R_{56}} \simeq \frac{\sigma_{\delta_i}}{S}\ , \tag{4}$$

where the last equality holds if $S^2 \gg 1$. This technique is ideally suited for LPA beams due to their intrinsically ultra-short (few-μm) length and typically large (∼10 kA) peak current. Thus, for FEL applications, $S \sim 10$ would allow for an order of magnitude improvement of the energy spread while maintaining a kA current. When high current is not required, such as in storage ring injectors, a more drastic energy spread reduction could be realized.

Eq. (1) shows that for ∼1 μm long and ∼1 % energy spread beams, $R_{56} \sim 1$ mm is sufficient for $S \sim 10$. As illustrated in Fig. 1, this dispersion could be generated by a symmetric magnetic chicane, where path length differences arise due to an energy-dependent transverse deflection. This results in $R_{56} = 2\theta^2(L_d + 2L_m/3)$ [49], where L_m and θ are, respectively, the magnet length and bending angle (for $\delta = 0$); and L_d is the distance between the central and outer dipoles.

When Eq. (3) is satisfied, Eq. (2) also yields that the final deviation of the average beam energy is given by

$$\langle \delta_f \rangle = \frac{\zeta_0}{R_{56}}\ . \tag{5}$$

This implies that, if $\zeta_0 = 0$, the final beam energy is stabilized to $\gamma_{\rm ref}$ regardless of its initial value. This stabilization can only be realized with an *active* dechirping medium, where ζ_0 can be controlled independently of the beam position. In order to achieve this, we propose here a so-called active plasma dechirper, a device where the dechirping fields are generated by a laser pulse split from the main LPA driver, and not by the electron beam itself. This is conceptually similar to a laser-plasma lens [50],

but aimed at the generation of longitudinal fields. The intrinsic synchronization between the LPA and APD pulses allows the arrival time of the APD driver to be adjusted with sufficient precision to ensure that $\zeta_0 = 0$. The impact that a timing jitter of the APD driver would have on the final beam energy stability can also be evaluated directly from Eq. (5). This yields that for $R_{56} \sim 1\,\mathrm{mm}$, maintaining a per-mille energy jitter requires a timing jitter $\lesssim 10\,\mathrm{fs}$, a level of precision which has been experimentally demonstrated [51].

The APD consists of a plasma source inside which a tightly focused laser pulse excites a trailing wakefield. When the peak normalized vector potential of the driver is sufficiently high, $a_0 \gtrsim 2$, large electron cavitation occurs and a strong wakefield with a uniform accelerating slope is generated (cf. Fig 2(a)). The length of this cavity is approximately given by the plasma wavelength $\lambda_p = 2\pi/k_p$, where $k_p = (n_p e^2/m_e \epsilon_0 c^2)^{1/2}$ and n_p are the plasma electron wavenumber and density and ϵ_0 is the vacuum permittivity. The longitudinal extension of the stretched beam should fit within this cavity. As depicted in Fig. 1, this can be ensured by placing a slit in the center of the chicane for collimating particles beyond a maximum, $\delta_{\max}$, and minimum, $\delta_{\min}$, energy deviation. For a total beam extension $\lesssim \lambda_p/2$, this yields a condition $\lambda_p \gtrsim 2\,(\delta_{\max} - \delta_{\min}) R_{56}$, which determines the maximum plasma density in the APD. The field slope $\mathcal{E}'$ can be estimated from the non-linear cold fluid equation [52] for the wakefield potential, ψ, behind the driver, $\mathcal{E}' = \partial_\zeta^2 \psi = -k_p^2\,(1 - 1/(1+\psi)^2)/2$. At ζ_0, which occurs around the center of the cavity, the wakefield potential is maximum and given approximately by $\psi_0 \sim k_p^2 w_0^2/4$ [53], where w_0 is the spot size of the laser at focus. This implies that $\mathcal{E}' \sim -k_p^2\,(1 - 1/(1 + k_p^2 w_0^2/4)^2)/2$ around ζ_0. Coupled with Eq. (3), this expression allows for an estimation of the required dechirper length, under the assumption that $w \sim w_0$ throughout the dechirper. Relative to the laser Rayleigh length, $Z_R = \pi w_0^2/\lambda_0$ [52], the dechirper length is found to be $L/Z_R = \gamma_{\mathrm{ref}}\, R_{56}^{-1}\, \lambda_0\, g(k_p w_0)$, where λ_0 is the laser wavelength and $g(x) = 2(4+x^2)^2/\pi x^4(8+x^2)$. For $R_{56} = 1\,\mathrm{mm}$, $\gamma_{\mathrm{ref}} = 10^3$ and $\lambda_0 = 800\,\mathrm{nm}$, this expression yields $k_p w_0 \gtrsim 1$ for ensuring $L \lesssim Z_R$ (i.e. $w \sim w_0$). Under this condition, no external guiding is required and a compact, mm-long APD can be realized. This scales favorably to higher energies, requiring only a small increase to $k_p w_0 \gtrsim 2.6$ for $\gamma_{\mathrm{ref}} = 10^4$.

To demonstrate the capabilities of the presented concept, a set of start-to-end simulations of the beam decompression and APD have been carried out. The simulations start from a 6D Gaussian electron beam with parameters representing the current state-of-the-art [15, 35], featuring an energy of 500 MeV with an energy spread and energy jitter of 1 % rms. The simulated beamline follows the design outlined in Fig. 1, and aims at improving the beam energy spread and stability by at least an order of magnitude. The beam capture, transport and

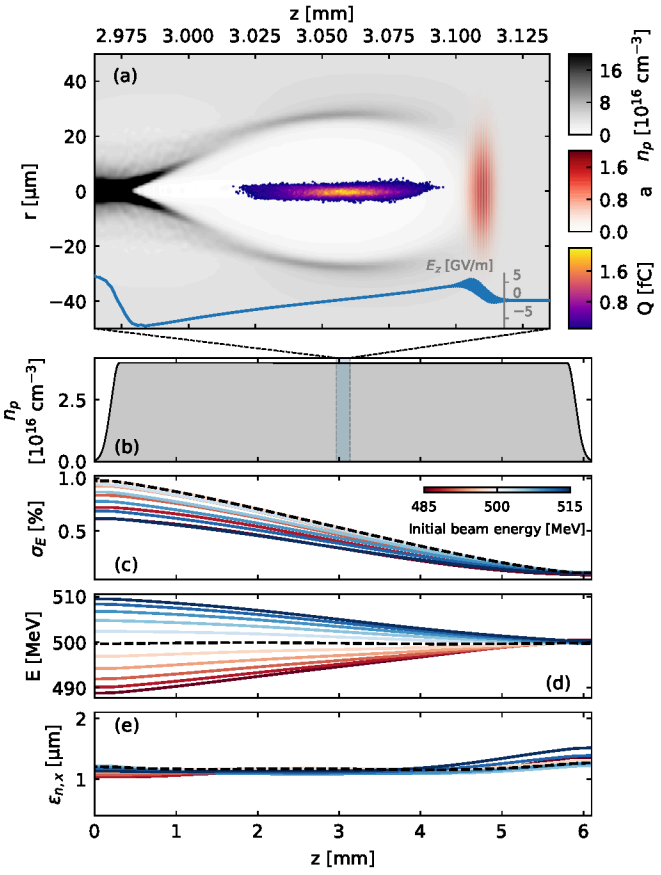

FIG. 2. (a) Plasma wakefields and electron beam at the center of the APD. (b) Density profile of the APD. (c), (d) and (e) show, respectively, the evolution of the rms energy spread, average energy and normalized emittance along the APD of beams with an initial energy deviation between −3 % and 3 %. The dashed lines show the reference case at 500 MeV. The differences in the initial energy spread arise due to charge loss in the chicane slit for strongly off-energy beams.

focus is performed by two active plasma lenses [54] placed 10 cm apart from the virtual LPA and the APD. Compared to the use of conventional magnets, this minimizes chromatic emittance growth [55] and simplifies the simulation setup. In practice, conventional transport lines using advanced chromaticity correction techniques could also be realized [56]. The simulations of the plasma elements have been performed with the quasi-3D particle-in-cell code FBPIC, while the chicane has been simulated with the OCELOT tracking code, including the effects of 3D space charge and 1D coherent synchrotron radiation (CSR). Hundreds of simulations have been performed to comprehensively study the energy stability of the setup.

The initial LPA beams have a typical normalized emittance $\epsilon_n = 1\,\mu\mathrm{m}$, a divergence of ∼0.5 mrad, a FWHM duration of 7 fs and a charge of 10 pC, resulting in a ∼1.3 kA peak current. The active plasma lenses provide a gradient of $800\,\mathrm{T\,m^{-1}}$ over a length of 2 cm and a plasma density of $10^{15}\,\mathrm{cm^{-3}}$. In order to achieve a per-

mille energy spread and jitter, a chicane with $S = 13$ has been used. From Eq. (1), this requires $R_{56} = 1.16\,\mathrm{mm}$, which is generated by a compact 1.6 m long chicane with $L_d = 30\,\mathrm{cm}$, $L_m = 20\,\mathrm{cm}$ and $\theta = 36.7\,\mathrm{mrad}$. The chicane includes a collimating slit with a total horizontal aperture of 1 mm for filtering particles with an energy deviation above $\pm 3\,\%$. The APD operates with a plasma density of $4 \times 10^{16}\,\mathrm{cm}^{-3}$ and has a plateau length of 5.5 mm with two short 0.3 mm Gaussian ramps at the entrance and exit. The APD driver is a bi-Gaussian pulse with $a_0 = 2$, $\lambda_0 = 0.8\,\mu\mathrm{m}$, $w_0 = 24\,\mu\mathrm{m}$, a FWHM duration of 25 fs, and an energy of 2 J.

More than 300 simulations with the prescribed energy jitter have been performed to study the performance of the scheme. Fig. 2 shows a detailed view of the beam evolution within the APD, including the wakefield structure at the center of the dechirper. The decompressed beam fits well within the plasma wake, and is positioned so that Eq. (5) ensures a final energy of 500 MeV. The effectiveness of this can be seen in Figs. 2(c)-(e), which show the energy spread, mean energy and emittance of a subset of 11 beams with $-3\,\% \leq \langle \delta_i \rangle \leq 3\,\%$. All of them converge to the final target energy while reducing the energy spread to $\lesssim 0.1\,\%$. The emittance is not significantly affected, experiencing an average growth of 7.1 % due to transverse beam loading, since the blowout is not fully cavitated of plasma electrons. APDs thus have a clear advantage over passive dechirpers in terms of central energy stabilization, while offering a large dechirping strength ($\sim$78 GeV mm^{-1} m^{-1} in the present case) and emittance preservation.

The energy compression and stabilization of the LPA beams, as seen in Fig. 3, results in a drastic improvement of the average beam energy spread and rms central energy jitter, which are reduced from 1 % to only 0.10 % and 0.024 %, respectively. This is a degree of stability orders of magnitude beyond current state-of-the-art. The impact of a timing jitter between the LPA and APD drivers has also been evaluated (cf. Fig. 3(c)). For a 10 fs rms jitter, larger than experimentally expected [51], a significantly reduced energy jitter of 0.26 % is still achieved. This is in full agreement with Eq. (5), and showcases the robustness of the concept.

In addition to the energy stabilization, this scheme offers larger charge tolerance than previous work [24] owing to the bunch stretching (and peak current reduction) in the chicane. This minimizes beam-loading effects in the APD, which could otherwise perturb the linearity of the dechirping fields, while still allowing for an efficient LPA with optimal beam loading. The charge tolerance of the APD has been tested by performing the same scan as in Figs. 3(a)-(b) for beams with a charge of 5 pC, 10 pC, 20 pC, 30 pC and 50 pC, keeping the rest of the setup unchanged. The resulting cumulative energy spectra are shown in Fig. 4. A sub-permille energy jitter is achieved in all cases, with a value between 0.024 % (5 pC) and 0.074 % (50 pC). The final average energy spread also varies between 0.079 % (5 pC) and 0.43 % (50 pC) due to the increased beam loading in the APD. Thus, even for a beam charge 5 times larger than the design value, an excellent stabilization is achieved, albeit with less effective energy spread reduction. Higher charge tolerance can be realized by re-optimizing the beam line. For the same 50 pC beam, a final energy spread of 0.18 % can be obtained by using a 2.5 mm APD with an increased density of $8 \times 10^{16}\,\mathrm{cm}^{-3}$, a chicane with $S = 10$, and the same APD laser driver but focused to $w_0 = 22\,\mu\mathrm{m}$.

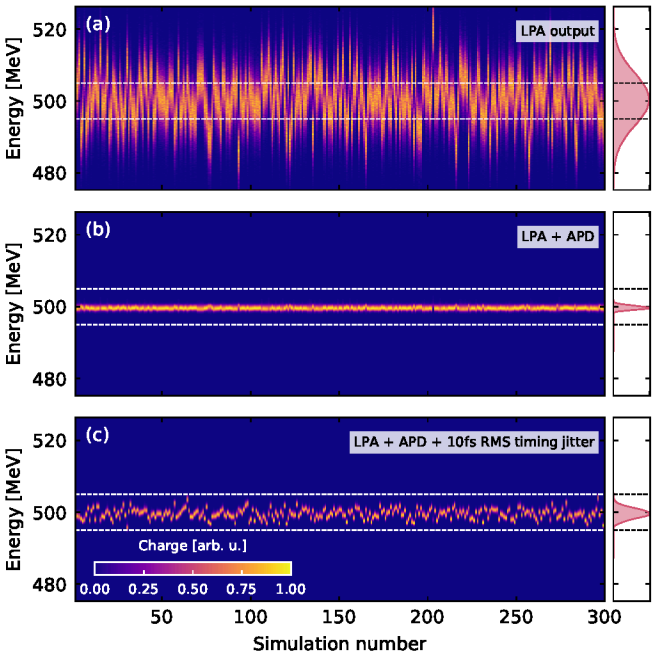

FIG. 3. Energy spectrum of 300 simulated beams with an initial 1 % rms energy jitter and energy spread. (a) Initial spectrum of the Gaussian beam emulating the LPA output. (b) Final spectrum after lengthening and active dechirping. (c) Same as (b) but with a 10 fs rms timing jitter in the APD driver. The dashed lines represent a $\pm 1\,\%$ energy deviation.

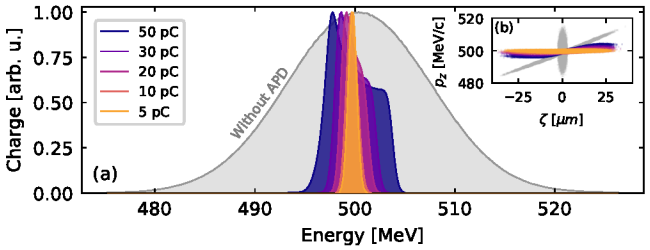

FIG. 4. (a) Energy spectrum of the LPA output with and without an APD for different values of the beam charge. Each curve is the projection of 300 simulations with an initial 1 % rms energy jitter. (b) Final longitudinal phase space of beams with $\langle \delta_i \rangle = 0$. Higher charge can lead to non-linearities due to beam loading. For reference, the phase space at the LPA and chicane exit is also included (gray).

In conclusion, we have shown that bunch decompression in combination with an active plasma dechirper can effectively correct the energy output of an LPA. Start-to-end simulations demonstrate that an unprecedented beam energy spread and energy jitter in the permille to sub-permille range could be achieved with this technique, using currently-available laser technology. This would enable LPAs as compact beam sources for future storage rings or free-electron lasers.

The authors would like to thank S. Jalas, M. Kirchen and A. Maier for useful discussions. This research was supported in part through the Maxwell computational resources operated at Deutsches Elektronen-Synchrotron DESY, Hamburg, Germany. The authors gratefully acknowledge the Gauss Centre for Supercomputing e.V. (www.gauss-centre.eu) for funding this project by providing computing time through the John von Neumann Institute for Computing (NIC) on the GCS Supercomputer JUWELS [57] at Jülich Supercomputing Centre (JSC).

* angel.ferran.pousa@desy.de

[1] T. Tajima and J. M. Dawson, Laser electron accelerator, Phys. Rev. Lett. **43**, 267 (1979).

[2] K. Nakajima, Towards a table-top free-electron laser, Nat. Phys. **4**, 92 (2008).

[3] S. Hillenbrand, R. Assmann, A.-S. Müller, O. Jansen, V. Judin, and A. Pukhov, Study of laser wakefield accelerators as injectors for synchrotron light sources, Nucl. Instrum. Methods Phys. Res. A **740**, 153 (2014), proceedings of the first European Advanced Accelerator Concepts Workshop 2013.

[4] S. P. D. Mangles, C. D. Murphy, Z. Najmudin, A. G. R. Thomas, J. L. Collier, A. E. Dangor, E. J. Divall, P. S. Foster, J. G. Gallacher, C. J. Hooker, *et al.*, Monoenergetic beams of relativistic electrons from intense laser–plasma interactions, Nature **431**, 535 (2004).

[5] C. Geddes, C. Toth, J. Van Tilborg, E. Esarey, C. Schroeder, D. Bruhwiler, C. Nieter, J. Cary, and W. Leemans, High-quality electron beams from a laser wakefield accelerator using plasma-channel guiding, Nature **431**, 538 (2004).

[6] J. Faure, Y. Glinec, A. Pukhov, S. Kiselev, S. Gordienko, E. Lefebvre, J.-P. Rousseau, F. Burgy, and V. Malka, A laser–plasma accelerator producing monoenergetic electron beams, Nature **431**, 541 (2004).

[7] W. P. Leemans, B. Nagler, A. J. Gonsalves, C. Tóth, K. Nakamura, C. G. R. Geddes, E. Esarey, C. B. Schroeder, and S. M. Hooker, Gev electron beams from a centimetre-scale accelerator, Nature Physics **2**, 696 (2006).

[8] W. P. Leemans, A. J. Gonsalves, H.-S. Mao, K. Nakamura, C. Benedetti, C. B. Schroeder, C. Tóth, J. Daniels, D. E. Mittelberger, S. S. Bulanov, J.-L. Vay, C. G. R. Geddes, and E. Esarey, Multi-gev electron beams from capillary-discharge-guided subpetawatt laser pulses in the self-trapping regime, Phys. Rev. Lett. **113**, 245002 (2014).

[9] A. J. Gonsalves, K. Nakamura, J. Daniels, C. Benedetti, C. Pieronek, T. C. H. de Raadt, S. Steinke, J. H. Bin, S. S. Bulanov, J. van Tilborg, C. G. R. Geddes, C. B. Schroeder, C. Tóth, E. Esarey, K. Swanson, L. Fan-Chiang, G. Bagdasarov, N. Bobrova, V. Gasilov, G. Korn, P. Sasorov, and W. P. Leemans, Petawatt laser guiding and electron beam acceleration to 8 gev in a laser-heated capillary discharge waveguide, Phys. Rev. Lett. **122**, 084801 (2019).

[10] O. Lundh *et al.*, Few femtosecond, few kiloampere electron bunch produced by a laser–plasma accelerator, Nat. Phys. **7**, 219 (2011).

[11] S. Fritzler, E. Lefebvre, V. Malka, F. Burgy, A. E. Dangor, K. Krushelnick, S. P. D. Mangles, Z. Najmudin, J.-P. Rousseau, and B. Walton, Emittance measurements of a laser-wakefield-accelerated electron beam, Phys. Rev. Lett. **92**, 165006 (2004).

[12] E. Brunetti, R. Shanks, G. Manahan, M. Islam, B. Ersfeld, M. Anania, S. Cipiccia, R. Issac, G. Raj, G. Vieux, *et al.*, Low emittance, high brilliance relativistic electron beams from a laser-plasma accelerator, Phys. Rev. Lett. **105**, 215007 (2010).

[13] R. Weingartner, S. Raith, A. Popp, S. Chou, J. Wenz, K. Khrennikov, M. Heigoldt, A. R. Maier, N. Kajumba, M. Fuchs, B. Zeitler, F. Krausz, S. Karsch, and F. Grüner, Ultralow emittance electron beams from a laser-wakefield accelerator, Phys. Rev. ST Accel. Beams **15**, 111302 (2012).

[14] S. Corde, K. Ta Phuoc, G. Lambert, R. Fitour, V. Malka, A. Rousse, A. Beck, and E. Lefebvre, Femtosecond x rays from laser-plasma accelerators, Rev. Mod. Phys. **85**, 1 (2013).

[15] M. Kirchen, S. Jalas, P. Messner, P. Winkler, T. Eichner, L. Hübner, T. Hülsenbusch, L. Jeppe, T. Parikh, M. Schnepp, and A. R. Maier, Optimal beam loading in a laser-plasma accelerator, Phys. Rev. Lett. **126**, 174801 (2021).

[16] S. van der Meer, *Improving the power efficiency of the plasma wakefield accelerator*, Tech. Rep. CERN-PS-85-65-AA. CLIC-Note-3 (CERN, Geneva, 1985).

[17] M. Tzoufras, W. Lu, F. S. Tsung, C. Huang, W. B. Mori, T. Katsouleas, J. Vieira, R. A. Fonseca, and L. O. Silva, Beam loading in the nonlinear regime of plasma-based acceleration, Phys. Rev. Lett. **101**, 145002 (2008).

[18] K. V. Lotov, Efficient operating mode of the plasma wakefield accelerator, Phys. Plasmas **12**, 053105 (2005).

[19] J. P. Couperus, R. Pausch, A. Köhler, O. Zarini, J. M. Krämer, M. Garten, A. Huebl, R. Gebhardt, U. Helbig, S. Bock, K. Zeil, A. Debus, M. Bussmann, U. Schramm, and A. Irman, Demonstration of a beam loaded nanocoulomb-class laser wakefield accelerator, Nat. Commun. **8**, 487 (2017).

[20] C. Lin, J. van Tilborg, K. Nakamura, A. J. Gonsalves, N. H. Matlis, T. Sokollik, S. Shiraishi, J. Osterhoff, C. Benedetti, C. B. Schroeder, C. Tóth, E. Esarey, and W. P. Leemans, Long-range persistence of femtosecond modulations on laser-plasma-accelerated electron beams, Phys. Rev. Lett. **108**, 094801 (2012).

[21] A. Ferran Pousa, A. Martinez de la Ossa, and R. W. Assmann, Intrinsic energy spread and bunch length growth in plasma-based accelerators due to betatron motion, Sci. Rep. **9**, 17690 (2019).

[22] R. Brinkmann, N. Delbos, I. Dornmair, M. Kirchen, R. Assmann, C. Behrens, K. Floettmann, J. Grebenyuk,

M. Gross, S. Jalas, T. Mehrling, A. Martinez de la Ossa, J. Osterhoff, B. Schmidt, V. Wacker, and A. R. Maier, Chirp mitigation of plasma-accelerated beams by a modulated plasma density, Phys. Rev. Lett. **118**, 214801 (2017).

[23] G. G. Manahan, A. F. Habib, P. Scherkl, P. Delinikolas, A. Beaton, A. Knetsch, O. Karger, G. Wittig, T. Heinemann, Z. M. Sheng, J. R. Cary, D. L. Bruhwiler, J. B. Rosenzweig, and B. Hidding, Single-stage plasma-based correlated energy spread compensation for ultrahigh 6d brightness electron beams, Nat. Commun. **8**, 15705 (2017).

[24] A. Ferran Pousa, A. Martinez de la Ossa, R. Brinkmann, and R. W. Assmann, Compact multistage plasma-based accelerator design for correlated energy spread compensation, Phys. Rev. Lett. **123**, 054801 (2019).

[25] R. D'Arcy, S. Wesch, A. Aschikhin, S. Bohlen, C. Behrens, M. J. Garland, L. Goldberg, P. Gonzalez, A. Knetsch, V. Libov, A. M. de la Ossa, M. Meisel, T. J. Mehrling, P. Niknejadi, K. Poder, J.-H. Röckemann, L. Schaper, B. Schmidt, S. Schröder, C. Palmer, J.-P. Schwinkendorf, B. Sheeran, M. J. V. Streeter, G. Tauscher, V. Wacker, and J. Osterhoff, Tunable plasma-based energy dechirper, Phys. Rev. Lett. **122**, 034801 (2019).

[26] V. Shpakov, M. P. Anania, M. Bellaveglia, A. Biagioni, F. Bisesto, F. Cardelli, M. Cesarini, E. Chiadroni, A. Cianchi, G. Costa, M. Croia, A. Del Dotto, D. Di Giovenale, M. Diomede, M. Ferrario, F. Filippi, A. Giribono, V. Lollo, M. Marongiu, V. Martinelli, A. Mostacci, L. Piersanti, G. Di Pirro, R. Pompili, S. Romeo, J. Scifo, C. Vaccarezza, F. Villa, and A. Zigler, Longitudinal phase-space manipulation with beam-driven plasma wakefields, Phys. Rev. Lett. **122**, 114801 (2019).

[27] Y. P. Wu, J. F. Hua, Z. Zhou, J. Zhang, S. Liu, B. Peng, Y. Fang, Z. Nie, X. N. Ning, C.-H. Pai, Y. C. Du, W. Lu, C. J. Zhang, W. B. Mori, and C. Joshi, Phase space dynamics of a plasma wakefield dechirper for energy spread reduction, Phys. Rev. Lett. **122**, 204804 (2019).

[28] Y. Wu, J. Hua, C.-H. Pai, W. An, Z. Zhou, J. Zhang, S. Liu, B. Peng, Y. Fang, S. Zhou, X. Xu, C. Zhang, F. Li, Z. Nie, W. Lu, W. Mori, and C. Joshi, Near-ideal dechirper for plasma-based electron and positron acceleration using a hollow channel plasma, Phys. Rev. Applied **12**, 064011 (2019).

[29] S. Antipov, S. Baturin, C. Jing, M. Fedurin, A. Kanareykin, C. Swinson, P. Schoessow, W. Gai, and A. Zholents, Experimental demonstration of energy-chirp compensation by a tunable dielectric-based structure, Phys. Rev. Lett. **112**, 114801 (2014).

[30] F. Mayet, R. Assmann, and F. Lemery, Longitudinal phase space synthesis with tailored 3d-printable dielectric-lined waveguides, Phys. Rev. Accel. Beams **23**, 121302 (2020).

[31] K. Bane and G. Stupakov, Corrugated pipe as a beam dechirper, Nuclear Instruments and Methods in Physics Research Section A: Accelerators, Spectrometers, Detectors and Associated Equipment **690**, 106 (2012).

[32] F. Fu, R. Wang, P. Zhu, L. Zhao, T. Jiang, C. Lu, S. Liu, L. Shi, L. Yan, H. Deng, C. Feng, Q. Gu, D. Huang, B. Liu, D. Wang, X. Wang, M. Zhang, Z. Zhao, G. Stupakov, D. Xiang, and J. Zhang, Demonstration of nonlinear-energy-spread compensation in relativistic electron bunches with corrugated structures, Phys. Rev. Lett. **114**, 114801 (2015).

[33] C. G. Schroer and H. DESY Dt. Elektr.-Synchr., *PETRA IV: upgrade of PETRA III to the Ultimate 3D X-ray microscope. Conceptual Design Report*, edited by R. Roehlsberger, E. Weckert, R. Wanzenberg, I. Agapov, R. Brinkmann, and W. Leemans (Deutsches Elektronen-Synchrotron DESY, Hamburg, 2019) pp. 259 pages : illustrations, diagrams.

[34] A. R. Maier, N. M. Delbos, T. Eichner, L. Hübner, S. Jalas, L. Jeppe, S. W. Jolly, M. Kirchen, V. Leroux, P. Messner, M. Schnepp, M. Trunk, P. A. Walker, C. Werle, and P. Winkler, Decoding sources of energy variability in a laser-plasma accelerator, Phys. Rev. X **10**, 031039 (2020).

[35] S. Jalas, M. Kirchen, P. Messner, P. Winkler, L. Hübner, J. Dirkwinkel, M. Schnepp, R. Lehe, and A. R. Maier, Bayesian optimization of a laser-plasma accelerator, Phys. Rev. Lett. **126**, 104801 (2021).

[36] L. Rovige, J. Huijts, I. Andriyash, A. Vernier, V. Tomkus, V. Girdauskas, G. Raciukaitis, J. Dudutis, V. Stankevic, P. Gecys, M. Ouille, Z. Cheng, R. Lopez-Martens, and J. Faure, Demonstration of stable long-term operation of a kilohertz laser-plasma accelerator, Phys. Rev. Accel. Beams **23**, 093401 (2020).

[37] Z.-H. He, B. Hou, V. Lebailly, J. A. Nees, K. Krushelnick, and A. G. R. Thomas, Coherent control of plasma dynamics, Nat. Commun. **6**, 7156 (2015).

[38] Z.-H. He, B. Hou, G. Gao, V. Lebailly, J. A. Nees, R. Clarke, K. Krushelnick, and A. G. R. Thomas, Coherent control of plasma dynamics by feedback-optimized wavefront manipulation, Phys. Plasmas **22**, 056704 (2015).

[39] S. J. D. Dann, C. D. Baird, N. Bourgeois, O. Chekhlov, S. Eardley, C. D. Gregory, J.-N. Gruse, J. Hah, D. Hazra, S. J. Hawkes, C. J. Hooker, K. Krushelnick, S. P. D. Mangles, V. A. Marshall, C. D. Murphy, Z. Najmudin, J. A. Nees, J. Osterhoff, B. Parry, P. Pourmoussavi, S. V. Rahul, P. P. Rajeev, S. Rozario, J. D. E. Scott, R. A. Smith, E. Springate, Y. Tang, S. Tata, A. G. R. Thomas, C. Thornton, D. R. Symes, and M. J. V. Streeter, Laser wakefield acceleration with active feedback at 5 hz, Phys. Rev. Accel. Beams **22**, 041303 (2019).

[40] A. R. Maier, A. Meseck, S. Reiche, C. B. Schroeder, T. Seggebrock, and F. Grüner, Demonstration scheme for a laser-plasma-driven free-electron laser, Phys. Rev. X **2**, 031019 (2012).

[41] W. A. Gillespie and M. G. Kelliher, The energy compressor at the glasgow 170 mev electron linac, Nucl. Instrum. Methods **184**, 285 (1981).

[42] R. Lehe, M. Kirchen, I. A. Andriyash, B. B. Godfrey, and J.-L. Vay, A spectral, quasi-cylindrical and dispersion-free particle-in-cell algorithm, Comput. Phys. Commun. **203**, 66 (2016).

[43] I. Agapov, G. Geloni, S. Tomin, and I. Zagorodnov, Ocelot: A software framework for synchrotron light source and fel studies, Nucl. Instrum. Methods Phys. Res. A **768**, 151 (2014).

[44] A. Ferran Pousa, *Novel Concepts and Theoretical Studies for High-Quality Plasma-Based Accelerators*, Dissertation, Universität Hamburg, Hamburg (2020).

[45] C. M. S. Sears, E. Colby, R. J. England, R. Ischebeck, C. McGuinness, J. Nelson, R. Noble, R. H. Siemann, J. Spencer, D. Walz, T. Plettner, and R. L. Byer, Phase

stable net acceleration of electrons from a two-stage optical accelerator, Phys. Rev. ST Accel. Beams **11**, 101301 (2008).

[46] F. Mayet, R. W. Aßmann, R. Brinkmann, J. Bödewadt, U. Dorda, W. Kuropka, C. Lechner, B. Marchetti, and J. Zhu, A concept for phase-synchronous acceleration of microbunch trains in dla structures at sinbad, in *Proc. of 8th International Particle Accelerator Conference (IPAC17)*, edited by V. R. Schaa, G. Arduini, J. Pranke, M. Seidel, and M. Lindroos (2017).

[47] A. F. Pousa, R. Assmann, R. Brinkmann, and A. M. de la Ossa, External injection into a laser-driven plasma accelerator with sub-femtosecond timing jitter, Journal of Physics: Conference Series **874**, 012032 (2017).

[48] A. Ferran Pousa, R. W. Assmann, and A. Martinez de la Ossa, VisualPIC: A New Data Visualizer and Post-Processor for Particle-in-Cell Codes, in *Proc. of 8th International Particle Accelerator Conference (IPAC17)* (2017).

[49] A. W. Chao, K. H. Mess, M. Tigner, and F. Zimmermann, eds., *Handbook of accelerator physics and engineering* (World Scientific, Hackensack, USA, 2013).

[50] C. Thaury, E. Guillaume, A. Döpp, R. Lehe, A. Lifschitz, K. Ta Phuoc, J. Gautier, J.-P. Goddet, A. Tafzi, A. Flacco, F. Tissandier, S. Sebban, A. Rousse, and V. Malka, Demonstration of relativistic electron beam focusing by a laser-plasma lens, Nature Communications **6**, 6860 (2015).

[51] S. Steinke, J. van Tilborg, C. Benedetti, C. G. R. Geddes, C. B. Schroeder, J. Daniels, K. K. Swanson, A. J. Gonsalves, K. Nakamura, N. H. Matlis, B. H. Shaw, E. Esarey, and W. P. Leemans, Multistage coupling of independent laser-plasma accelerators, Nature **530**, 190 (2016).

[52] E. Esarey, C. B. Schroeder, and W. P. Leemans, Physics of laser-driven plasma-based electron accelerators, Rev. Mod. Phys. **81**, 1229 (2009).

[53] W. Lu, C. Huang, M. Zhou, M. Tzoufras, F. S. Tsung, W. B. Mori, and T. Katsouleas, A nonlinear theory for multidimensional relativistic plasma wave wakefields, Phys. Plasmas **13**, 056709 (2006).

[54] J. van Tilborg, S. Steinke, C. G. R. Geddes, N. H. Matlis, B. H. Shaw, A. J. Gonsalves, J. V. Huijts, K. Nakamura, J. Daniels, C. B. Schroeder, C. Benedetti, E. Esarey, S. S. Bulanov, N. A. Bobrova, P. V. Sasorov, and W. P. Leemans, Active plasma lensing for relativistic laser-plasma-accelerated electron beams, Phys. Rev. Lett. **115**, 184802 (2015).

[55] M. Migliorati, A. Bacci, C. Benedetti, E. Chiadroni, M. Ferrario, A. Mostacci, L. Palumbo, A. R. Rossi, L. Serafini, and P. Antici, Intrinsic normalized emittance growth in laser-driven electron accelerators, Phys. Rev. ST Accel. Beams **16**, 011302 (2013).

[56] C. A. Lindstrøm, Staging of plasma-wakefield accelerators, Phys. Rev. Accel. Beams **24**, 014801 (2021).

[57] Jülich Supercomputing Centre, JUWELS: Modular Tier-0/1 Supercomputer at the Jülich Supercomputing Centre, Journal of large-scale research facilities **5**, 10.17815/jlsrf-5-171 (2019).